Arrays of point absorber wave energy converters with effects of a vertical wall.

KARA, Fuat

Prospects of Mechanical Engineering & Technology

Juniper Publishers
key to the Researchers

Research Article
Volume 1 Issue 1 - November 2022

Prospects Mech Eng Technol

Arrays of Point Absorber Wave Energy Converters with Effects of a Vertical Wall

Fuat Kara*

Sheffield Hallam University, Howard Street, Sheffield, S1 1WB, UK

Submission: October 22, 2022; **Published:** November 25, 2022

***Corresponding author**: Fuat Kara, Sheffield Hallam University, Howard Street, Sheffield, S1 1WB, UK

Abstract

The in-house transient wave-multibody numerical tool of ITU-WAVE is used to predict the wave power absorption with Wave Energy Converters (WECs) arrays in front of a vertical wall. The analyses of hydrodynamic radiation and exciting forces are approximated solving boundary integral equation with time marching scheme. The method of images is used to predict the perfect reflection of incident waves from a vertical wall. The constructive or destructive effect with different array configurations can be measured with mean interaction factor which determines the performances of WECs. The vertical wall effect plays significant role over hydrodynamic parameters as the radiation and exciting forces show quite different behaviors in the case of WECs with and without vertical wall in an array system. When the performance and wave power absorption with WECs arrays in front of vertical are compare, it is shown with numerical experience that WECs in front of vertical wall have much greater effects on wave power absorption and performances. This is mainly due to standing and nearly trapped waves between a vertical wall and WECs arrays in addition to strong interactions between WECs. The analytical and other numerical results are used to validate the numerical results of the present ITU-WAVE numerical results for different hydrodynamic parameters in an array system which shows satisfactory agreements.

Keywords: Boundary Integral Equation; Mean Interaction Factor; Method of Images; Transient Wave Green Function

Introduction

Wave energy from ocean waves can be absorbed with or without a coastal structures effect (e.g., a vertical wall) using isolated, linear, square, or rectangular WECs arrays. The efficiency of these options depends on the geometries of WECs and WECs array configurations, control strategies to maximize the absorb wave power [1], Power-Take-Off (PTO) systems, incoming wave heading angles, single mode of motion (e.g., heave or pitch) or multimode (e.g., heave and pitch). In addition to these parameters, in the case of WECs arrays in front of a vertical wall, the efficiency also depends on the separation distance between WECs [2] as well as a vertical wall and WECs. Although the installations, operations, and maintenances of WECs arrays at the offshore environment increase the overall cost significantly, the overall cost can be reduced by integrating WECs arrays with other coastal structures or placing them in front of them. As expected, the significant amount of wave power can be absorbed with WECs arrays compared to isolated WEC. This is mainly due to the hydrodynamic interactions between a vertical wall and WECs arrays as well as nearly trapped waves in the gap of array configurations [3].

The behaviors and performance of WECs in front of a vertical wall are studied both experimentally and numerically to define the effect of hydrodynamic interactions between a vertical wall and WECs arrays. The separation distances between a vertical wall and WECs as well as between WECs arrays play significant role on the maximum wave power absorption and performance of the array systems due to vertical wall effects [4]. The wave interaction and nearly trapped waves in the gap of WECs as well as a vertical wall and WECs can be used to increase the competitiveness and enhance the efficiency of array system. The performances of WEC arrays are studied with options of integrating or placing them in front of other maritime structures using different configurations including stationary and floating systems (e.g., Oscillating Water Column, Overtopping, oscillating buoys) [5].

Method of images assuming infinite vertical wall length is used in the present paper to predict the time dependent diagonal and interaction IRFs of exciting forces, which are the superposition of diffraction and Froude-Krylow forces, and radiation forces for 1x5, 2x5, 3x5, 4x5 and 5x5 sphere WECs arrays in front of a vertical wall at sway and heave modes. Fourier transform of IRFs is then used to obtain the frequency dependent exciting force amplitude as well as radiation added-mass and damping coefficients. These frequency dependent hydrodynamic parameters are then compared with other published numerical and analytical results for the validation of the present three-dimensional ITU-WAVE numerical results. The absorbed wave power, which are the functions of the hydrodynamic exciting and radiation forces, is directly predicted in time domain taking the average of instantaneous wave power signals. The contribution of transient effects on numerical results for wave power prediction is avoided by using only last half of the instantaneous wave power signals.

Materials and Methods

The hydrodynamic performances of WECs arrays in time domain are solved assuming that fluid is inviscid and incompressible, and its flow is irrotational such that there are no lifting effects and fluid separation. These assumptions on fluid and its flow result in using the potential theory and implicitly also mean that the time dependent flow velocity $\vec{v}(\vec{x},t)$ can be represented as the gradient of the velocity potential $\vec{v}(\vec{x},t)=\nabla\Phi(\vec{x},t)$. The use of potential theory also means that Laplace equation $\nabla^2\Phi(\vec{x},t)=0$ dictates the solutions of the time dependent velocity potentials $\Phi(\vec{x},t)$.

Equation of motion of arrays

The time dependent equation of motion of WECs arrays in front of a vertical wall in Equation (1) is the functions of acceleration relevant to inertia terms, hydrostatic restoring forces, and time dependent hydrodynamic restoring forces and exciting force parameters [6]. The effects of the incident waves result in the pressure changes around WECs arrays which cause the oscillations of WECs. The oscillating WECs in an array system generates the radiated waves on free surface which are presented by the convolution integral on the left-hand side of Equation (1) whilst effects of incident and diffracted waves are presented with convolution integral on the right-hand side of Equation (1).

$$\Sigma_{k=1}^{6}(M_{kk_i}+a_{kk_i})\ddot{x}_{k_i}(t)+(b_{kk_i}+B_{PTO-kk_i})\dot{x}_{k_i}(t)+(C_{kk_i}+c_{kk_i}+C_{PTO-kk_i})x_{k_i}(t)+\int_0^t d\tau K_{kk_i}(t-\tau)\dot{x}_{k_i}(\tau)=\int_{-\infty}^{\infty} d\tau K_{kD_i}(t-\tau)\zeta(\tau) \quad (1)$$

where upper boundary of sum k=1,2, 3…,6 represents the rigid modes of motions of surge, sway, heave, roll, pitch, and yaw respectively whilst index i=1,2, 3…, N is for number of WECs in an array system. $x_k(t)=(1,2,3,\ldots,N)^T, \dot{x}_k(t)$ and $\ddot{x}_k(t)$, where dots represent time derivatives, is used for displacements, velocities, and accelerations, respectively. M_{kk} is the inertia mass matrix whilst C_{kk} is the hydrostatic restoring coefficients in Equation (2) m and C are the inertia mass and restoring coefficient of an isolated WEC respectively. As the same radius R is used for all spheres in WECs arrays, the restoring force and inertia mass of each WEC are the same $C_1=C_2=\cdots=C_N=C$ and $m_1=m_2=\cdots=m_N=m$ respectively.

$$M_{kk}=\begin{pmatrix} m_1 & \cdots & 0 \\ \vdots & \ddots & \vdots \\ 0 & \cdots & m_N \end{pmatrix}, C_{kk}\begin{pmatrix} c_1 & \cdots & 0 \\ \vdots & \ddots & \vdots \\ 0 & \cdots & C_N \end{pmatrix} \quad (2)$$

The time and frequency independent restoring coefficient C_{kk}, damping coefficient b_{kk} and infinite added mass a_{kk} coefficients in Equation (3) depend on geometry and are relevant to displacement, velocity, and acceleration, respectively. The interaction terms are represented with off-diagonal terms whilst the diagonal terms represent the contribution of each WEC in an array system. IRF $K_{kk}(t)$,which is the function of the time and geometry, represent the force on k-th body due to the impulsive velocity of k-th body. The oscillations of WECs in an array system cause the disturbance of free surface which is known as the memory effect of the fluid responses. The convolution integral on the left-hand side of Equation (1) are used to represent the memory effect and the effect of the wave damping [7].

$$K_{kk}(t)=\begin{pmatrix} K_{11} & \cdots & K_{1N} \\ \vdots & \ddots & \vdots \\ K_{N1} & \cdots & K_{NN} \end{pmatrix}, a_{kk}=\begin{pmatrix} a_{11} & \cdots & a_{1N} \\ \vdots & \ddots & \vdots \\ a_{N1} & \cdots & a_{NN} \end{pmatrix}$$

$$b_{kk}=\begin{pmatrix} b_{11} & \cdots & b_{1N} \\ \vdots & \ddots & \vdots \\ b_{N1} & \cdots & b_{NN} \end{pmatrix}, C_{kk}=\begin{pmatrix} c_{11} & \cdots & c_{1N} \\ \vdots & \ddots & \vdots \\ c_{N1} & \cdots & c_{NN} \end{pmatrix} \quad (3)$$

The time dependent exciting force IRFs $K_{kE}(t)=(K_{1E},K_{2E},K_{3E},\ldots,K_{NE})^T$ on the k-th body is due to impulsive incident wave elevation $\zeta(t)$,which is a uni-directional incoming wave system with arbitrary heading angles, as presented in Equation (4). The superposition of diffraction and Froude-Krylov IRFs results in the exciting forces and moments $K_{kE}(t)$ in time on the right-hand side of Equation (1) [8].

$$F_{kE}(t)=\int_{-\infty}^{\infty} d\tau K_{kE_i}(t-\tau)\zeta(\tau) \quad (4)$$

The elements of PTO in Equation (5) are the time independent and frequency dependent wave damping coefficient B_{PTO-kk}

How to cite this article: Fuat Kara. Arrays of Point Absorber Wave Energy Converters with Effects of a Vertical Wall. Prospects Mech Eng Technol. 2022; 1(1): 555553.

matrix and C_{PTO-kk} which is the time and frequency independent restoring coefficient matrix. It is theoretically known that the maximum wave power is absorbed at the resonant frequency [9].

It is the reason that the diagonal elements of PTO matrix B_{PTO-kk} in Equation (5) are selected as the wave damping at the resonant frequency at which the natural frequency of isolated WEC and incident wave excitation frequency are equal. For the simplicity purpose, the off-diagonal terms of PTO matrix, which represent the wave damping due to cross-interaction between WECs in an array system, are considered zero. The elements of are C_{PTO-kk} considered zero for heave mode while for sway mode, the diagonal elements of C_{PTO-kk} are taken the same as hydrostatic restoring coefficient of heave mode to have the same natural frequency and displacement in both heave and sway modes. In this case, it would be possible to compare heave and sway motions and power variables directly to decide which modes of motion are more effective and efficient for power absorption.

$$B_{PTO-kk} = \begin{pmatrix} B_{iso}(\omega_n) & \cdots & 0 \\ \vdots & \ddots & \vdots \\ 0 & \cdots & B_{iso}(\omega_n) \end{pmatrix}$$

$$C_{PTO-kk} = \begin{pmatrix} C_1 & \cdots & 0 \\ \vdots & \ddots & \vdots \\ 0 & \cdots & C_N \end{pmatrix} \quad (5)$$

where the natural frequency of each isolated WEC is given with w_n. The time marching scheme with fourth order Runge-Kutta method [10] can be used to solve the equation of motion Equation (1) after determination of PTO damping B_{PTO-kk} restoring matrices, and inertia mass matrix M_{kk}. The time and frequency independent added mass at infinite wave frequency a_{kk}, wave damping b_{kk} and restoring c_{kk} coefficients are also input for Equation (1) In addition, Equation (1) at each time step requires the hydrodynamic restoring or wave damping which is represented with convolution integral on the left-hand side of Equation (1) and is the function of the radiation IRFs and velocity of WECs. Furthermore, the exciting force at each time step is also required and represented with convolution integral on the right-hand side of Equation (1).

Instantaneous and mean absorbed wave power

The instantaneous wave energy $P_{ins_{k_i}}(t)$ is converted to useful electrical energy at each mode of motion from each WEC in an array system with PTO system. $P_{ins_{k_i}}(t)$ is presented in Equation (6) and is the functions of exciting force, radiation force, and velocity of each WEC placed in front of a vertical wall.

$$P_{ins_{k_i}}(t) = [F_{exc_{k_i}}(t) + F_{rad_{k_i}}(t)] \cdot \dot{x}_{k_i}(t) \quad (6)$$

where $F_{exc_{k_i}}(t)$ in Equation(7) being time dependent exciting force due to incident and diffracted waves and $F_{rad_{k_i}}(t)$ in Equation (8) being radiation force due to oscillation of each WEC in an array system whilst the velocities of each WEC in front of a vertical wall are presented with $\dot{x}_{k_i}(t)$ [1,2].

$$F_{exc_{k_i}}(t) = F_{k_i}(t) = \int_{-\infty}^{\infty} d\tau K_{kD_i}(t-\tau)\zeta(\tau) \quad (7)$$

$$F_{rad_{k_i}}(t) = -a_{kk_i}\ddot{x}_{k_i}(t) - b_{kk_i}\dot{x}(t) - c_{kk_i}x_{k_i}(t) - \int_0^t d\tau K_{kk_i}(t-\tau)\dot{x}_{k_i}(\tau) \quad (8)$$

The product of time dependent exciting force $F_{exc_{k_i}}(t)$ in Eq. (7) and WEC velocity $\dot{x}_{k_i}(t)$ results in the absorbed total exciting wave power $P_{exc_{k_i}}(t) = F_{exc_{k_i}}(t) \cdot \dot{x}_{k_i}(t)$ from incident wave at any heading angles. The product of time dependent velocity $\dot{x}_{k_i}(t)$ and radiation force $F_{rad_{k_i}}(t)$ in Equation (8) results in radiation wave power $P_{rad_{k_i}}(t) = F_{rad_{k_i}}(t) \cdot \dot{x}_{k_i}(t)$ which is the power that is radiated back to sea. The absorbed mean wave power $\overline{P}_{ins_{k_i}}(t)$ with PTO system over a range of time T in Equation (9) is averaged to predict the absorbed useful wave power.

$$\overline{P}_{ins_{k_i}}(t) = \frac{1}{T}\int_0^T dt \cdot [F_{exc_{k_i}}(t) + F_{rad_{k_i}}(t)] \cdot \dot{x}_{k_i}(t) \quad (9)$$

The time dependent absorbed total mean wave power $\overline{P}_{T_K}$ in Equation (10) at mode of motion of k is the superposition of the mean wave power that is absorbed with each $i-th$ WEC in an array system in front of a vertical wall with N numbers of WECs.

$$\overline{P}_{T_K}(t) = \sum_{i=1}^{N} P_{ins_{k_i}}(t) \quad (10)$$

Mean interaction factor

The mean interaction factor $q_{mean,k}(\omega)$ at any incident wave frequency is used to measure the gain factor due to the interaction of WECs in an array system in front of a vertical wall. $q_{mean,k}(\omega)$ are the functions of wave power absorbed by N interacting WECs

How to cite this article: Fuat Kara. Arrays of Point Absorber Wave Energy Converters with Effects of a Vertical Wall. Prospects Mech Eng Technol. 2022; 1(1): 555553.

and an isolated WEC at any given heading angles. The constructive $(q_{mean,k}(\omega) > 1)$ and destructive $(q_{mean,k}(\omega) < 1)$ effects of mean interaction factor $q_{mean,k}(\omega)$ depend on the separation distance between WECs as well as a vertical wall and WECs, incident wave heading angles, geometry of WECs, and control strategies to improve the efficiency of WECs in an array system.

The frequency dependent mean interaction factor at any incident wave frequency in Equation (11) is given as the ratio of the sum of mean absorbed wave power with N number of WECs in an array system in front of a vertical wall to N times the mean absorbed wave power with an isolated WEC at the resonant frequency [11].

$$q_{mean,k}(\omega) = \frac{\overline{P}_{T_K}(\omega)}{N \times \overline{P}_{ins_{ko}}(\omega_n)} \quad (11)$$

where N is the number of WECs in an array system. The sum of the mean absorbed wave power at any mode of motion k is given with $\overline{P}_{T_K}(\omega)$ at any given incident wave frequency ω whilst the mean absorbed wave power with an isolated WEC is given with $\overline{P}_{ins_{ko}}(\omega_n)$ at the resonant frequency w_n.

Results and Discussions

The present numerical results of hydrodynamic parameters (e.g., exciting and radiation IRFs, exciting force amplitudes, added-mass and damping coefficients) and wave power absorptions from ocean waves with WECs in an array system with and without a vertical wall effect are predicted with in-house transient wave-multibody interaction computational code of ITU-WAVE [1,2,9,12-18].

Validation of ITU-WAVE numerical results

The position of WECs in front of a vertical wall is given with numbers (1, 2, 3, 4, 5). The heading angles are presented with β. d is the separation distance between WECs whilst wk is the separation distance between WECs and the vertical wall. In addition, the free surface is given with S_f whilst the surface at intersection between WECs and free surface is presented with Γ. WECs surface is given with S_b whilst the surface at infinity is presented with S_∞ in Figure 1a.

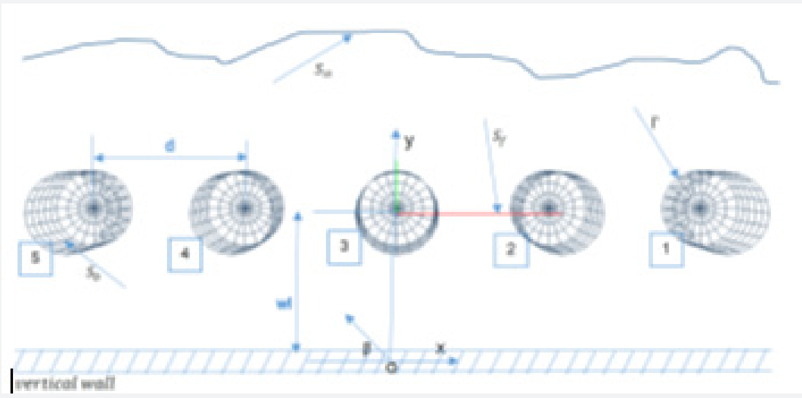

Figure 1: Coordinate system and surface of 1x5 WECs arrays in front of a vertical wall in xy-plane.

Figure 2(a) and Figure 2(b) show the dimensionless diagonal added-mass and damping coefficients in surge mode for 1x5 arrays of truncated vertical cylinder, respectively. The present ITU-WAVE numerical results are compared with analytical results of consolidates [19]. The comparison of present numerical results with analytical results shows satisfactory agreements.

The dimensionless sway exciting force amplitudes of square 2x2 arrays of truncated vertical cylinders at the incident wave angle of 270o are compared with the numerical results of Chatjigeorgiou [20] for WEC1 & WEC2 and WEC3 & WEC4 in Figure 3(a) and Figure 3(b) respectively. The present frequency dependent sway exciting force amplitudes of ITU-WAVE numerical results and those of Hatzigeorgiou [21] show satisfactory agreements.

The mean interaction factor of 2x5 arrays of vertical cylinder with hemisphere bottom in heave mode are presented in Figure 4 at heading angle 900. The predicted mean interaction factor of ITU-WAVE is compared with numerical result of McCallum *et al.* [22] in Figure (4). The present ITU-WAVE numerical result shows satisfactory agreement with that of McCallum et al. [22]. In addition to mean interaction factor, which is the sum of mean interaction

How to cite this article: Fuat Kara. Arrays of Point Absorber Wave Energy Converters with Effects of a Vertical Wall. Prospects Mech Eng Technol. 2022; 1(1): 555553.

factor of 1st row (WEC1-WEC5) and 2nd (WEC6-WEC10) row of 2x5 arrays system, the mean interaction factors of 1st and 2nd rows are also presented in Figure (5). The mean interaction factor of 2nd row, which is in the wake of 1st row that meets with the incident wave first, is greater and has more constructive effect compared to 1st row. This is mainly due to the strong hydrodynamic interactions and nearly trapped waves in the gap of 1st and 2nd rows of WECs in an array system. The mean interaction factor has maximum constructive effect at dimensionless natural frequency of 0.5 whilst it has destructive effect at about dimensionless incident wave frequency of 0.6. The mean interaction factor oscillates about q_{mean} = 1.0 up to dimensionless incident wave frequency of 0.4 which means that the same amount of wave energy from ocean waves is absorbed with isolated WECs and rectangle 2x5 arrays whilst mean interaction factor has mainly constructive effects at dimensionless higher incident wave frequencies.

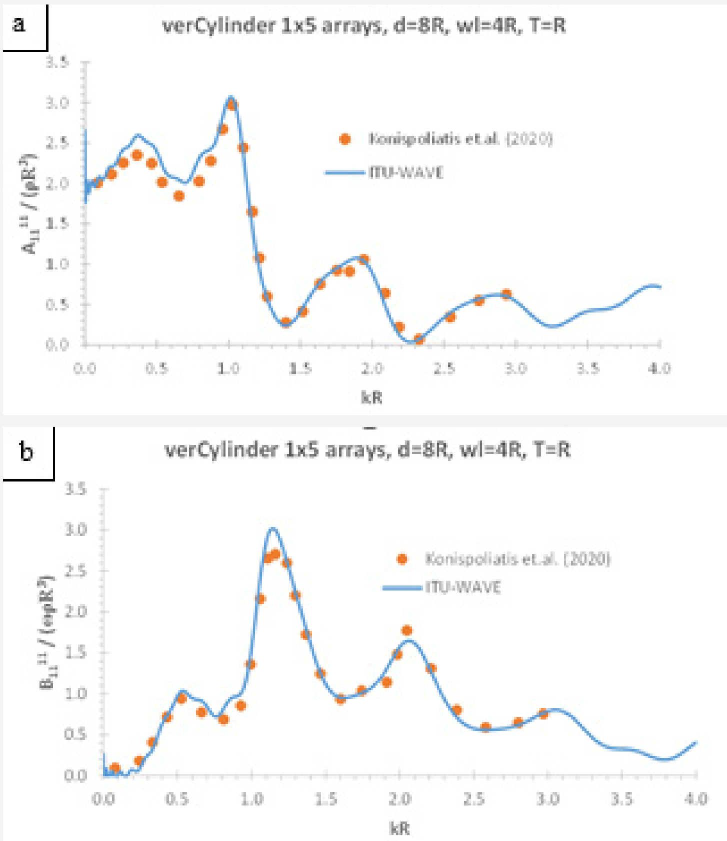

Figure 2: Surge dimensionless diagonal radiation force coefficients of WEC1; (a) added mass; (b) damping.

Radiation and exciting force IRFs

The dimensionless exciting force IRFs of 1x5 arrays of sphere with radius R are presented in Figure 6. The IRFs for WEC1 and WEC5 as well as WEC2 and WEC4 are the same due to symmetry of WECs with respect to heading angle of 90° for both with and without vertical wall effects. When with and without vertical wall effects are compared, the bandwidth of the IRFs with vertical wall effects are greater than that of without vertical wall effect. As the area under IRFs represents the available energy to be absorb with WECs, Figure 7 implicitly shows that more energy is available in the case of WECs arrays in front of a vertical wall due to wider bandwidths. The IRFs with vertical wall effects start to oscillate much earlier. This also implicitly means that WECs in an array system feel the effect of incident waves earlier in the case of WECs placed in front of a vertical wall.

The dimensionless heave exciting force IRFs at the middle of each row of 5x5 arrays of sphere without and with vertical wall effects are presented in Figure 8(a) and Figure8(b) respectively. Although the exciting force amplitudes of IRFs without and with vertical wall effects are approximately the same, the bandwidth of heave exciting force IRFs are greater in the case of WECs arrays in front of a vertical wall. This implicitly means that as mentioned before, more wave energy from ocean waves would be absorbed with WECs arrays placed in front of a vertical wall.

How to cite this article: Fuat Kara. Arrays of Point Absorber Wave Energy Converters with Effects of a Vertical Wall. Prospects Mech Eng Technol. 2022; 1(1): 555553.

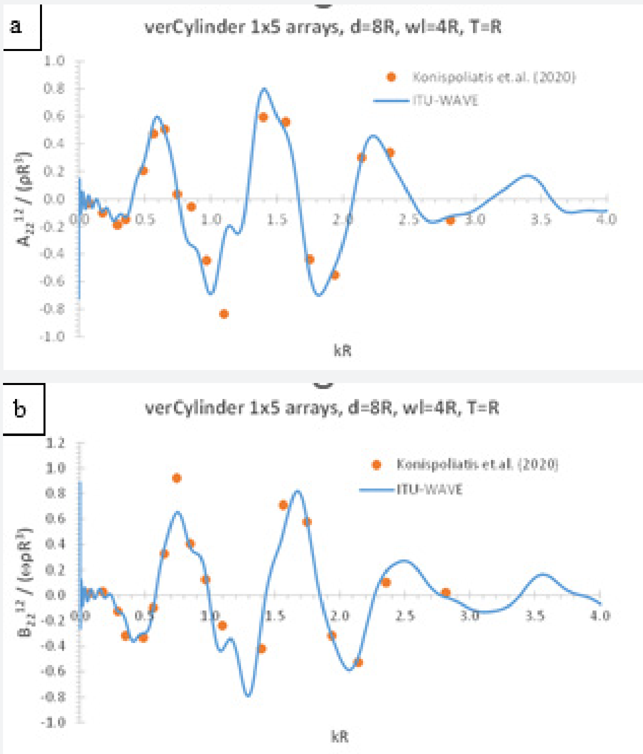

Figure 3: Sway dimensionless radiation interaction force coefficients between WEC1 and WEC2; (a) added mass; (b) damping coefficients.

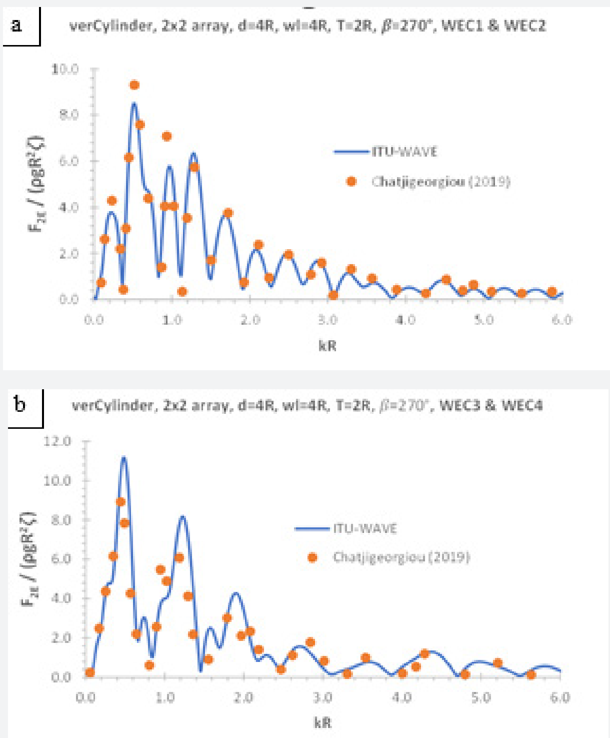

Figure 4: Sway nondimensional exciting force amplitudes; (a) WEC1 and WEC2; (b) WEC3 and WEC4.

How to cite this article: Fuat Kara. Arrays of Point Absorber Wave Energy Converters with Effects of a Vertical Wall. Prospects Mech Eng Technol. 2022; 1(1): 555553.

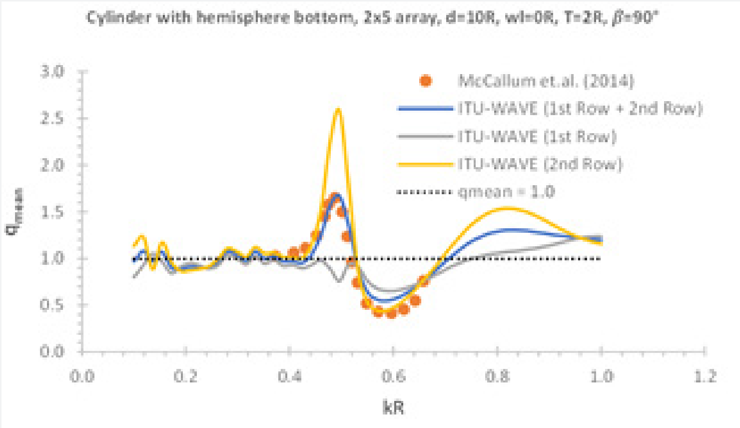

Figure 5: Mean interaction factor q_mean of rectangle 2x5 arrays of cylinder with hemisphere bottom without a vertical wall effect.

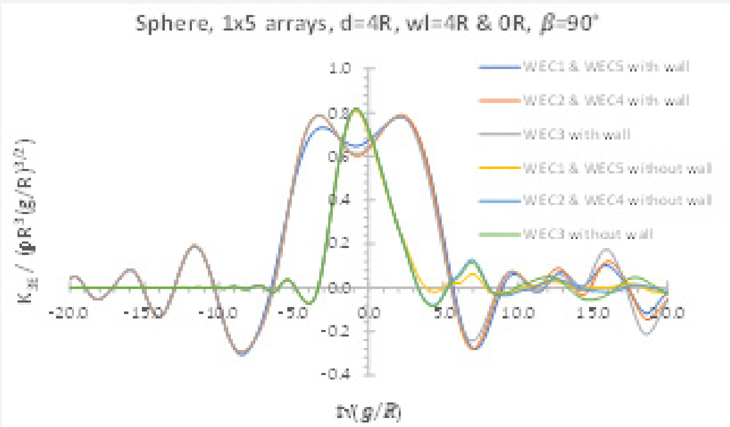

Figure 6: Heave dimensionless exciting force IRFs of 1x5 arrays of sphere with and without vertical wall effects.

The dimensionless heave radiation interaction IRFs of 1x5 arrays of sphere without and with vertical wall effects are presented in Figure 9(a) and Figure 9 (b) respectively. When radiation force IRFs with and without vertical wall effects are compared, the amplitude of IRFs with vertical wall effects are greater compared to those of without vertical wall effects at longer times although the amplitudes of interaction IRFs are approximately the same at lower times. As in the case of exciting IRFs, the greater amplitude of interaction radiation IRFs at larger times implicitly means that the more wave energy is available to be absorb. It may be also noticed that the interaction effects are greater at closer proximity of WECs whilst the greater interaction effects are shifted to longer times when the separation distances between WECs are increased.

Response Amplitude Operators (RAOs)

The sway and heave RAOs with 1x5 arrays of sphere in front of a vertical wall at heading angles 90° are presented in Figure 10(a) and Figure 10(b) respectively. The RAOs for WEC1 and WEC5 as well as WEC2 and WEC4 are the same due to the symmetry of WECs with respect to incident wave angle 90°. It may be also noticed that there are three resonance occurrences in both sway and heave modes, but magnitude of the resonances is finite.

The RAOs for sway and heave modes with 2x5 arrays in front of a vertical wall at heading angle 90° are presented in Figure 10(a), 10(b), 10(c) and 10(d) for 1st and 2nd rows of sway mode as well as 1st and 2nd rows of heave mode respectively. The incident wave meets 1st row WECs first, and 2nd row WECs are located at the wake of 1st row. There are three sway and six heave resonance

How to cite this article: Fuat Kara. Arrays of Point Absorber Wave Energy Converters with Effects of a Vertical Wall. Prospects Mech Eng Technol. 2022; 1(1): 555553.

occurrences for 1st row WECs. These resonances are finite which means that some of the wave energies are radiated back to sea due to oscillations of WECs in an array system. These resonance occurrences in sway and heave modes are due to hydrodynamic interaction in the wave motion between WECs as well as WECs and a vertical wall when the WECs in the array system are forced to oscillate on the free surface. The motions of the fluid between WECs as well as WECs and a vertical wall are strongly excited at frequencies corresponding to standing waves. An occurrence of complete reflection or complete transmission of incident waves is possible at standing wave frequencies where wave motion between WECs as well as WECs and a vertical wall is resonant [23]. The sway and heave RAOs for 2nd row WECs are greater than those of 1st row due to the standing and nearly trapped waves between gaps of WECs in an array system as well as WECs and a vertical wall. Both sway and heave RAOs of WEC1 and WEC5 as well as WEC2 and WEC4, which are the 1st row WECs in 2x5 rectangular arrays, are the same due to symmetry of WECs with respect to incident wave at heading angle 90° in Figure 10(a) and (c). It is also true that the RAOs of WEC6 and WEC10 as well as WEC7 and WEC9 in both sway and heave modes, which are the 2nd row WECs, are the same due to symmetry of WECs with respect to incident wave angle of 90° in Figure 10(b) and (d).

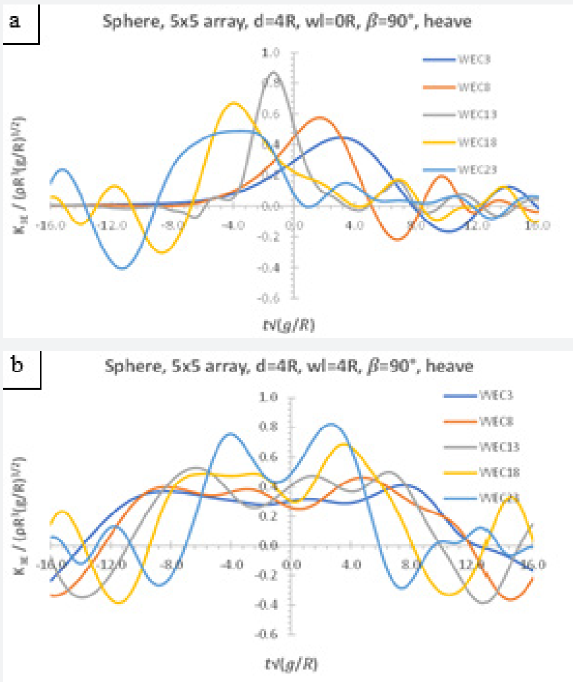

Figure 7: Heave dimensionless exciting force IRFs at the middle of each row of 5x5 arrays of sphere; (a) without vertical wall effect; (b) with vertical wall effect.

Absorbed wave power with 2x5 arrays

The sway and heave RAOs and absorbed wave power with an isolated sphere at heading angle 90° are presented in Figure 11(a) and 11 (b) respectively. As floating systems (e.g., sphere WEC) do not have the restoring force at sway mode, it is assumed in the present study that PTO restoring force coefficients at sway and heave modes are equal. This means both sway and heave modes have the same displacements which implies that the performances of sphere at both modes can be directly compared against each other. As it may be observed in Figure 11(b) and is theoretically known [24] that the maximum wave power is captured at resonant frequency at which natural frequency of sphere (w=1.38 rad/s) at both sway and heave modes are equal to incident wave frequency. It may be noticed in Figure 11(b) that more wave power is absorbed at resonant frequency at sway mode than heave mode. The absorption bandwidth in Figure 11(b) is much wider at sway mode at higher frequencies although heave mode absorbs more power at lower frequencies at which more wave energy is available to be absorb.

How to cite this article: Fuat Kara. Arrays of Point Absorber Wave Energy Converters with Effects of a Vertical Wall. Prospects Mech Eng Technol. 2022; 1(1): 555553.

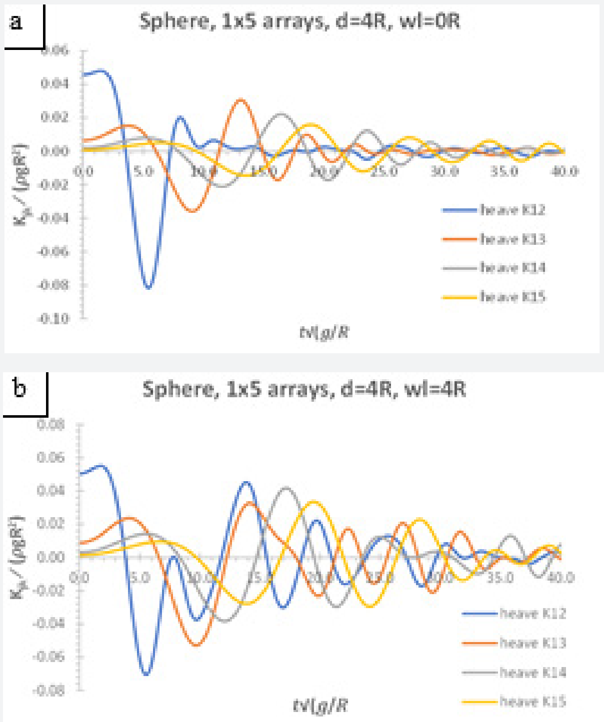

Figure 8: Heave dimensionless radiation interaction IRFs of 1x5 arrays of sphere; (a) without vertical wall effect; (b) with vertical wall effect.

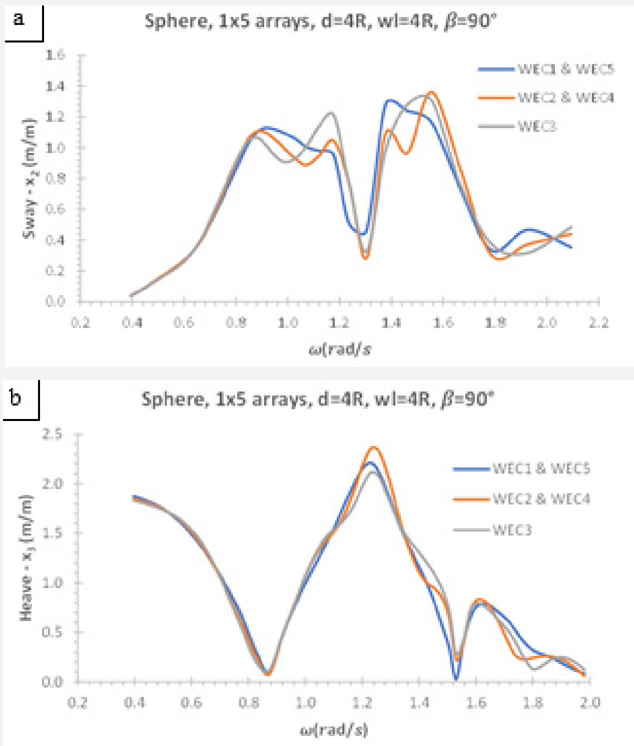

Figure 9: RAOs for each WEC in 1x5 arrays of sphere in front of a vertical wall; (a) sway; (b) heave.

How to cite this article: Fuat Kara. Arrays of Point Absorber Wave Energy Converters with Effects of a Vertical Wall. Prospects Mech Eng Technol. 2022; 1(1): 555553.

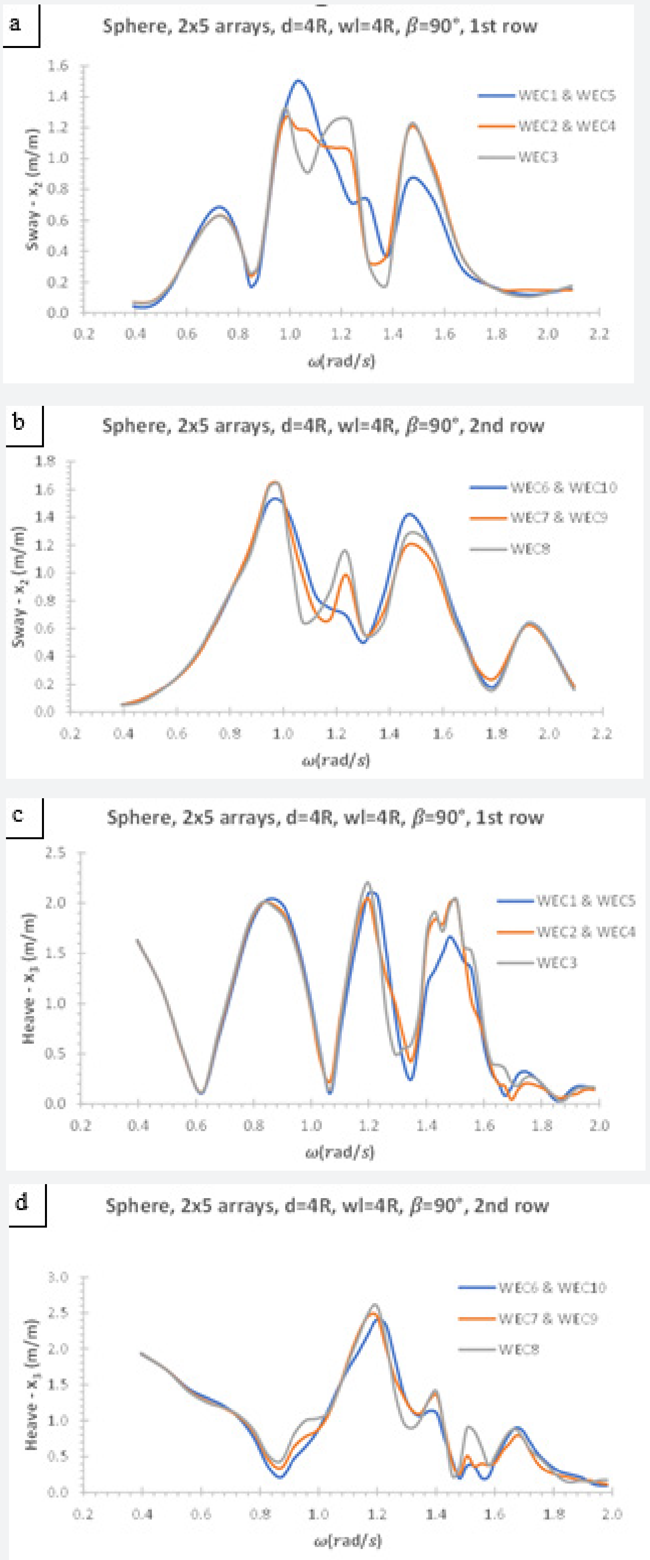

Figure 10: RAOs for each WEC in 2x5 arrays of sphere in front of a vertical wall; (a) sway – 1st row; (b) sway – 2nd row; (c) heave – 1st row; (d) heave – 2nd row.

How to cite this article: Fuat Kara. Arrays of Point Absorber Wave Energy Converters with Effects of a Vertical Wall. Prospects Mech Eng Technol. 2022; 1(1): 555553.

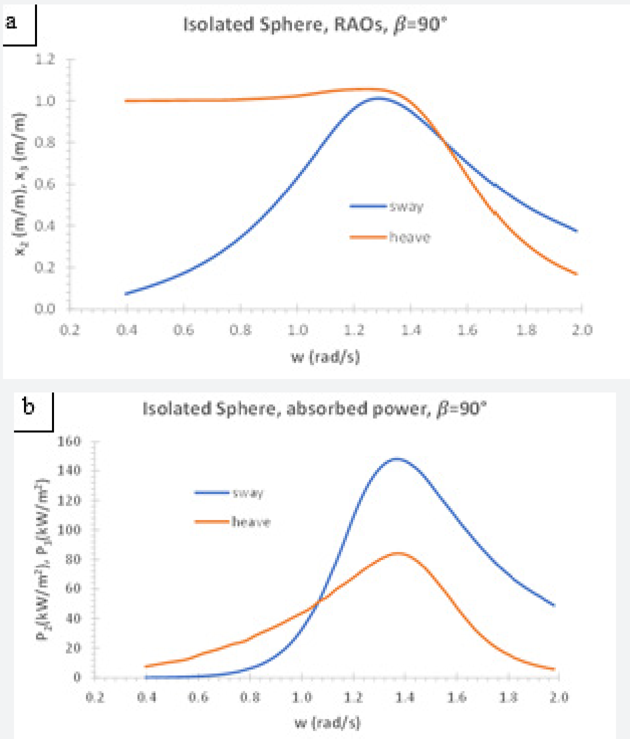

Figure 11: Isolated sphere with radius R in sway and heave modes; (a) RAOs; (b) absorbed power.

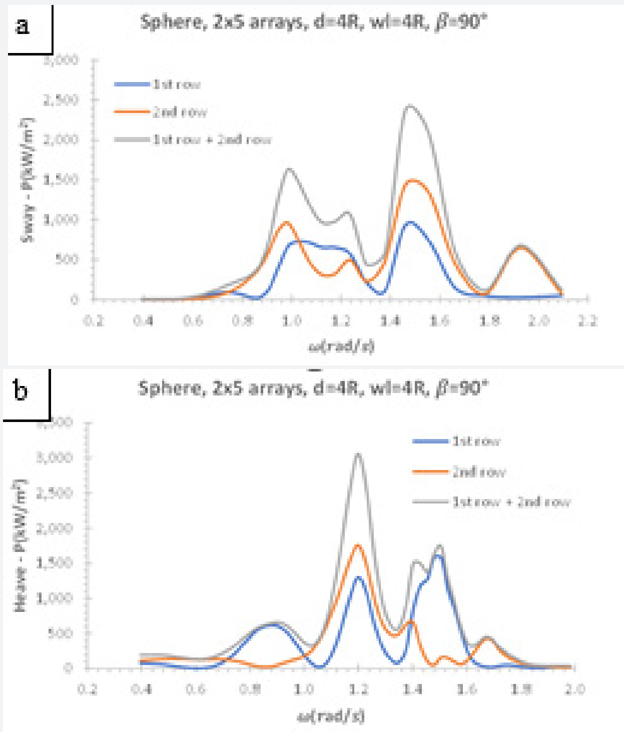

Figure 12: Absorbed wave power with 2x5 arrays of sphere in front of a vertical wall; (a) sway (b) heave mode.

 How to cite this article: Fuat Kara. Arrays of Point Absorber Wave Energy Converters with Effects of a Vertical Wall. Prospects Mech Eng Technol. 2022; 1(1): 555553.

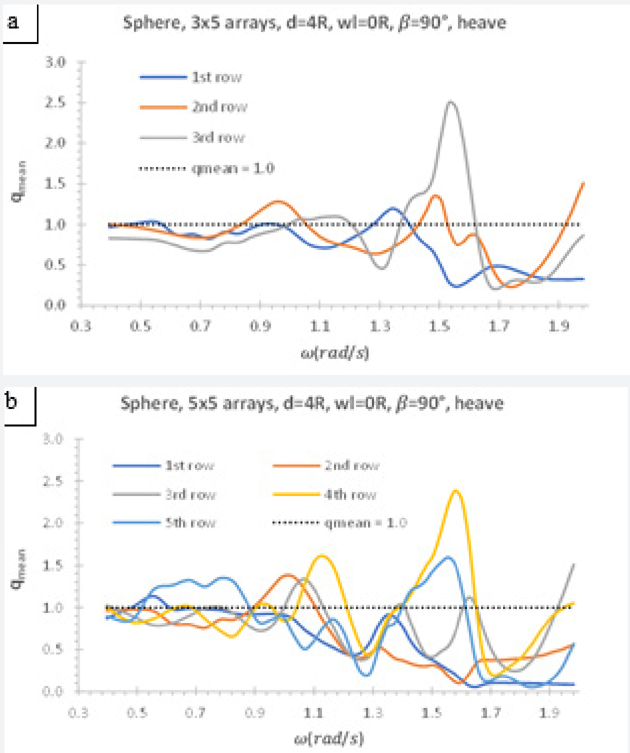

Figure 13: Mean interaction factors of sphere without vertical wall effect in heave mode; (a) 3x5; (b) 5x5 arrays.

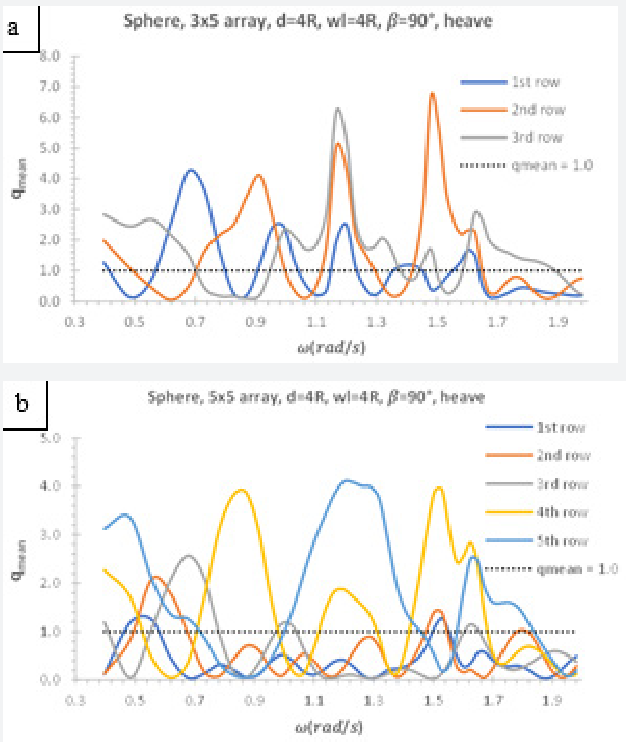

Figure 14: Mean interaction factors of each row of sphere in front of a vertical wall in heave mode; (a) 3x5 arrays; (b) 5x5 arrays.

How to cite this article: Fuat Kara. Arrays of Point Absorber Wave Energy Converters with Effects of a Vertical Wall. Prospects Mech Eng Technol. 2022; 1(1): 555553.

The absorbed wave power with 1st row, 2nd row and superpositions of 1st and 2nd rows using 2x5 arrays of sphere in front of a vertical wall at heading angles 90° is presented in Figure 12(a) and (b) for sway and heave modes respectively. The wave energy absorption in heave mode in Figure 12(b) is concentrated at wave frequencies of 1.2 and 1.5 rad/s whilst it is distributed in a range of incident wave frequencies with much wider frequency bandwidth in sway mode in Figure 12(a). The absorption with sway mode in Figure 12(a) are greater at around incident wave frequency of 1.0 and 1.5 rad/s. More wave power is absorbed in sway mode in Figure 12(a) with 2nd row WECs, which are at the wake of 1st row. The maximum wave power in Figure 12(b) is absorbed at the same incident wave frequency of 1.2 rad/s with 1st and 2nd row WECs with heave mode although 2nd row WECs absorb much greater wave power at incident wave frequency of 1.5 rad/s.

Mean interaction factors of arrays of sphere

Mean interaction factors q_mean of each row of sphere with 3x5 and 5x5 arrays are presented in Figure 13(a) and 13 (b) respectively. It can be observed that higher row numbers (e.g., 3rd row for 3x5 arrays and 4th and 5th rows for 5x5 arrays) has better constructive effects compared to lower row numbers especially at higher incident wave frequencies (e.g., 1st row) which meet with incident wave first. When the row numbers increase, the destructive effect of lower row numbers increases (e.g., 1st and 2nd rows). This may be noticed when mean interaction factor of 1st rows in Figures 13(a) and 13(b) are compared.

Mean interaction factors q_mean of sphere with 3x5 and 5x5 arrays in front of a vertical wall in heave mode are presented for each row in Figure 14(a) and 14 (b) respectively. It may be noticed that when the rows are closer to vertical wall, mean interaction factors are greater compared to the rows which are away from a vertical wall (e.g., 3rd and 2nd rows for 3x5 sphere arrays whilst 5th and 4th rows for 5x5 arrays). When the row numbers increase in an array system, the contributions of the rows away from a vertical wall to wave absorption in Figure 14(b) are mostly destructive (e.g., 1st, 2nd, and 3rd rows at especially higher frequencies).

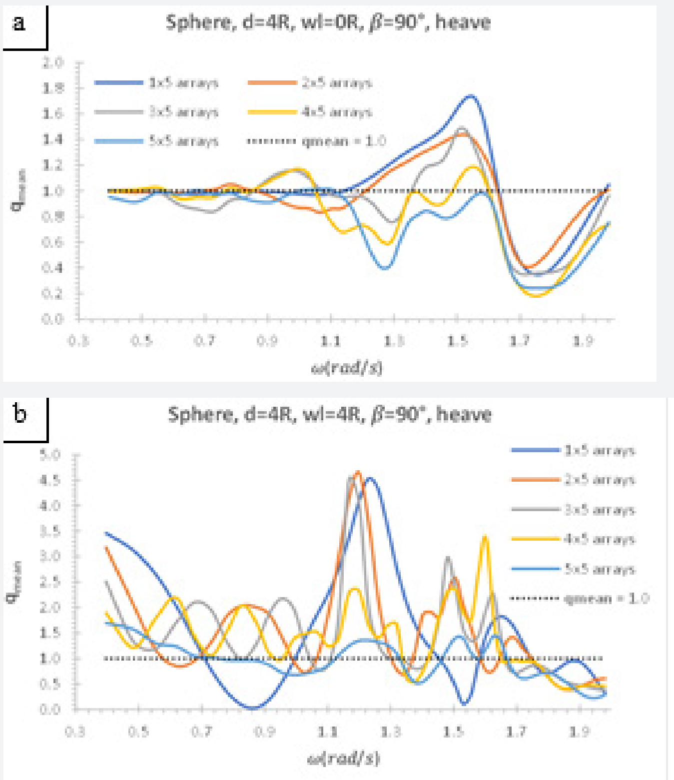

Figure15: Mean interaction factors of sphere in heave mode in a range of row numbers and 5 column numbers; (a) without a vertical wall effect; (b) with a vertical wall effect.

How to cite this article: Fuat Kara. Arrays of Point Absorber Wave Energy Converters with Effects of a Vertical Wall. Prospects Mech Eng Technol. 2022; 1(1): 555553.

Mean interaction factors without and with a vertical wall effect for sphere WECs of 1x5, 2x5, 3x5, 4x5 and 5x5 arrays in heave mode in a range of incident wave frequencies are presented in Figure 15(a) and 15(b) respectively. In the case of 1x5 arrays of sphere in front of a vertical wall, the behaviour of mean interaction factors shows constructive effect apart from about incident wave frequencies of 0.87 and 1.53 rad/s. When other array configurations in front of a vertical wall are considered, mean interaction factors of 2x5, 3x5, 4x5 and 5x5 arrays have the constructive effects in a range of the incident wave frequency up to 1.7 rad/s, however, after this incident wave frequency, mean interaction factors show destructive effects. The magnitudes of the constructive effects decrease with increasing row numbers at lower incident wave frequencies in Figure 15(b). Mean interaction factors of 2x5, 3x5, and 4x5 arrays in Figure 15(b) also show 2.2 times constructive effects up to incident wave frequency of 1.1 rad/s whilst the constructive effects of 1x5, 2x5, and 3x5 arrays reach up to 4.65 times at incident wave frequency of 1.2 rad/s. However, these constructive effects decrease up to 2.3 and 1.4 for 4x5 and 5x5 arrays at the same incident wave frequency of 1.2 rad/s respectively. In the case of arrays without a vertical wall effect, the dominant incident wave frequency is around 1.5 rad/s for constructive effect whilst it is around 1.75 rad/s for destructive effect. When with and without a vertical wall effect are compared, it can be clearly observed from Figure 15(a) and 15(b) that the magnitudes of the constructive effects of WECs arrays in front of a vertical wall in Figure 15(b) are much greater almost all range of incident wave frequencies compared to without a vertical wall effect in Figure 15(a).

Conclusion

The exploitation of the wave power absorption from ocean waves using WECs arrays with and without a vertical wall effect is analysed with in-house transient wave-multibody interaction computational tool of ITU-WAVE. The time dependent boundary integral equation method is used to solve the initial boundary value problem with time marching scheme whilst the perfect reflection of the incident waves from a vertical wall is predicted with method of images in ITU-WAVE numerical tool.

The nearly trapped and standing waves in the gap of WECs as well as WECs and a vertical wall in an array system play significant role for the maximum wave power absorption especially closer separation distances. It is found out by the numerical experiences that the mean interaction factors for all considered array systems are at least 2 times greater in the case of arrays in front of a vertical wall compared to arrays without a vertical wall effect. The constructive effect is also much greater than destructive effect in an array system in front of a vertical wall for all considered array systems.

References

1. Kara F (2010) Time Domain Prediction of Power Absorption from Ocean Waves with Latching Control. Renewable Energy 35(2):423-434.
2. Kara F (2016) Point absorber wave energy converter in regular and irregular waves with time domain analysis. International Journal of Marine Science and Ocean Technology 3(7): 74-85.
3. Mustapa MA, Yaakob OB, Ahmed YM, Rheem C.-K, Koh KK, et al. (2017) Wave energy device and breakwater integration: A review. Renewable and Sustainable Energy Reviews 77, 43–58.
4. Schay J, Bhattacharjee J, Soares CG (2013) Numerical Modelling of a Heaving Point Absorber in front of a Vertical Wall. In Proceedings of the ASME 32nd International Conference on Ocean, Offshore and Arctic Engineering, Nantes, France, P. 9–14.
5. Ning DZ, Zhao XL, Goteman M, Kang HG (2016) Hydrodynamic performance of a pile-restrained WEC-type floating breakwater an experimental study. Renew Energy 95:531-541.
6. Cummins WE (1962) The Impulse response function and ship motions. Shiffstechnik 9: 101-109.
7. Ogilvie TF (1964) Recent progress toward the understanding and prediction of ship motions. Proceedings of the 5th Symposium on Naval Hydrodynamics, Office of Naval Research, Washington, D.C.USA: 3-80.
8. King BW (1987) Time domain analysis of wave exciting forces on ships and bodies. PhD thesis, The University of Michigan, Ann Arbor Michigan USA.
9. Budal K, Falnes J (1976) Optimum operation of wave power converter. Internal Report, Norwegian University of Science and Technology.
10. Kara F (2016) Time Domain Prediction of Seakeeping Behaviour of Catamarans. International Shipbuilding Progress 62 (3-4): 161-187.
11. Thomas GP, Evans DV (1981) Arrays of three-dimensional wave-energy absorbers. Journal of Fluid Mechanics 108: 67-88.
12. Kara F (2021) Hydrodynamic performances of wave energy converters arrays in front of a vertical wall. Ocean Engineering 235: 109459.
13. Kara F (2021) Hydroelastic behaviour and analysis of marine structures. Journal of Sustainable Marine Structures 2: 14-24.
14. Kara F (2021) Application of time domain methods for marine hydrodynamic and hydroelasticity analyses of floating systems. Ships and Offshore Structures.
15. Kara F (2020) Multibody interactions of floating bodies with time domain predictions. Journal of Waterway, Port, Coastal and Ocean Engineering 146(5): 04020031.
16. Kara F (2017) Control of wave energy converters for maximum power absorptions with time domain analysis. Journal of Fundamentals of Renewable Energy and Applications 7(1): 1-8.
17. Kara F (2016) Time Domain Prediction of Power Absorption from Ocean Waves with Wave Energy Converters Arrays. Renewable Energy 92: 30-46.
18. Kara F (2011) Time Domain Prediction of Added Resistance of Ships. Journal of Ship Research 55(3): 163-184.
19. Konispoliatis DN (2020) Mavrakos SA and Katsaounis GM. Theoretical evaluation of the hydrodynamic characteristics of arrays of vertical axisymmetric floaters of arbitrary shape in front of a vertical breakwater. Journal of Marine Science and Engineering 8(1): 62.
20. Chatjigeorgiou IK (2019) Semi-analytical solution for the water wave diffraction by arrays of truncated circular cylinders in front of a vertical wall. Applied Ocean Research 88: 147-159.

21. McCallum P, Venugopal V, Forehand D, Sykes R. (2014) On the performance of an array of floating wave energy converters for different water depths. Proceedings of the ASME: 33 rd. International Conference on Ocean, Offshore and Arctic Engineering, 2014, OMEA2014, June 8-13, USA.

22. Newman JN (1974) Interactions of water waves with two closely spaced vertical obstacles. Journal of Fluid Mechanics 66(1): 97–106.

23. Evans DV (1975) A note on the total reflection or transmission of surface waves in the presence of parallel obstacles. Journal of Fluid Mechanics 67: 465–472.

24. Budal K (1976) Theory for absorption of wave power by a system of interacting bodies. Journal of Ship Research 21(4): 248-253.